

Acute Experimental Diabetes and Aortic Depressor Nerve Ultrastructural Morphometry: Effects of Insulin Treatment

Fabício Singaretti de Oliveira¹, Milena Menezes de Amorim^{2,3}, Jaci Airton Castania⁴, Helio Cesar Salgado⁴, Randy Alan Nessler³, Valéria Paula Sassoli Fazan^{2,3,5*}

¹Department of Animal Morphology and Physiology, School of Veterinary Medicine, State University of São Paulo, Jaboticabal, SP, Brazil

²Department of Neuroscience and Behavioral Neurosciences, School of Medicine of Ribeirão Preto, University of São Paulo, Ribeirão Preto, SP, Brazil

³Central Microscopy Research Facility, The University of Iowa, Iowa City, IA, USA

⁴Department of Physiology, School of Medicine of Ribeirão Preto, University of São Paulo, Ribeirão Preto, SP, Brazil

⁵Department of Surgery and Anatomy, School of Medicine of Ribeirão Preto, University of São Paulo, Ribeirão Preto, SP, Brazil

Abstract

Previous results from our laboratory showed myelinated fiber alterations in the aortic depressor nerve (ADN) from rats rendered diabetic for 15 days (short term). The ultrastructure and the acute effect of insulin treatment, particularly in the unmyelinated fibres of this nerve, were not yet investigated in this experimental model, being the aim of this work. Wistar rats received a single intravenous injection of streptozotocin (STZ – 40 mg/Kg) 15 days (N=7) before the experiments. Control animals (N=7) received vehicle (citrate buffer) and treated animals (n=6) received a subcutaneous injection of insulin (10 IU/Kg) on a daily basis beginning 3 days after the STZ injection. Under pentobarbital anaesthesia the ADNs were isolated and had their spontaneous activity recorded. Afterwards, proximal and distal segments of the nerves were prepared for transmission electron microscopy studies. Morphometry of the myelinated and unmyelinated fibres was carried out with the aid of computer software. Nerves from diabetic animals showed some unmyelinated fiber enlargement with signs of swelling and degeneration, and the Schwann cells mitochondria presented enlargement and clustering formation. On treated animals, an important thickening of the Schwann cells' basement membrane was present and some myelinated fibers showed thin myelin sheaths. The endoneurial blood vessels ultrastructure was preserved in all nerves from the three experimental groups. Myelinated axon area and diameter was significantly larger on insulin treated animals, compared to both, controls and acute diabetic groups, on both segments. No other differences were observed between groups for the myelinated or unmyelinated fibers morphometric parameters. Investigation of experimental models of diabetes in early or acute stage of the disease provide relevant information on the physiopathological mechanisms involved in the alterations present in patients with chronic diabetes and its complications. We suggest that insulin treatment alone might have a role on the morphological alterations present in diabetic neuropathy.

Keywords: Aortic depressor nerve; Acute diabetes; Insulin treatment; Morphometry; Ultrastructure

Introduction

Diabetes is a metabolic disorder of multiple etiologies caused by defects in insulin secretion, insulin action, or both, resulting in chronic hyperglycemia. Initial symptoms such as thirst, polyuria, and weight loss are unspecific and often not severe, or even absent. Thus, hyperglycemia sufficient to cause pathological associated or not to functional changes, may be present for a long time before the diagnosis is made. Neuropathy is a common complication of diabetes that accounts for a significant high morbidity [1]. Comi and Corbo [2] documented that one third of diabetic patients present some degree of neuropathy but a recent publication from the Centers for Disease Control and Prevention [3] indicated that this percent is much higher (up to 70%). Despite recent information about the mechanisms for many of the long term complications of diabetes, the exact pathogenesis of diabetic neuropathy remains unknown.

The literature is extensive on investigation of peripheral nervous system alterations in experimental models of diabetes (induced or genetic) but morphological alterations totally comparable to those that occur in the human diabetic neuropathy are not completely reproducible [4]. Nevertheless, it is expected that alterations observed in experimental models, especially in the early or acute cases, will be useful for a better understanding of the neuropathy development mechanisms [4]. Among the alterations on the peripheral nervous

system due to diabetes, the involvement of the autonomic nervous system is the least understood. The autonomic diabetic neuropathy is often under diagnosed and the most common clinical manifestation is sexual dysfunction. Functional alterations of the autonomic cardiovascular reflexes have been demonstrated in clinical and animal models [5-8] and most of the reports about altered baroreflex sensitivity attribute this alteration to the diabetic vagal (efferent) neuropathy.

The aortic depressor nerve (ADN) is unique in rodents because it contains only baroreceptor afferents (sensory) fibers [9,10]. The ADN (afferent arm of the baroreflex) ultrastructure was recently explored in a long term experimental model of diabetes [11] with important

***Corresponding author:** Valéria Paula Sassoli Fazan, Department of Surgery and Anatomy, School of Medicine of Ribeirão Preto, USP, Av. Bandeirantes 3900, Ribeirão Preto, SP, Brazil and Central Microscopy Research Facility, The University of Iowa, Iowa City, IA, USA, Tel: +55 16 3602-4634; Fax: +55 16 3633-0017; E-mail: vpsfazan@yahoo.com.br, vpsfazan@gmail.com

Received: September 03, 2014; **Accepted:** September 23, 2014; **Published:** September 25, 2014

Citation: Oliveira FS, Amorim MM, Castania JA, Salgado HC, Nessler RA, et al. (2014) Acute Experimental Diabetes and Aortic Depressor Nerve Ultrastructural Morphometry: Effects of Insulin Treatment. *Anat Physiol* 4: 159. doi:10.4172/2161-0940.1000159

Copyright: © 2014 Oliveira FS et al. This is an open-access article distributed under the terms of the Creative Commons Attribution License, which permits unrestricted use, distribution, and reproduction in any medium, provided the original author and source are credited.

morphological alterations being demonstrated. Nevertheless, the ultrastructure investigation of the ADN in acute diabetes was not previously reported, being the purpose of this study.

Materials and Methods

All described experimental procedures adhered to the Guide for the Care and Use of Laboratory Animals prepared by the National Academy of Sciences and published by the National Institutes of Health (Copyright©1996 by the National Academy of Sciences), and were approved by the Institutional Ethics Committee for Animal Research (CETEA–Comitê de Ética em Experimentação Animal, protocol number 220/2005). All effort was made to minimize the number of animals used.

Male Wistar rats, from the animal care facility of the Campus of Ribeirão Preto (University of São Paulo), were housed in plastic cages with free access to tap water and rat chow throughout the experiment. Diabetes induction was performed through a single injection of streptozotocin (STZ) (40 mg/kg, Sigma Chemical Co., St. Louis, MO, USA) into the penile vein 15 days (N=7) before the experiments. Nonfasting blood glucose (mg/dL) was determined by means of a glucose analyzer (Beckman Instruments Inc., Brea, CA, USA) on the third day after STZ injection and at the time of the experiments. Animals with glucose levels higher than 350 mg/dL, observed on the 3rd day after the STZ injection, were considered diabetic and included in the study. Insulin treated animals (N=6) received a subcutaneous injection of 9 IU/kg of NPH (highly purified mixed) insulin (Biolin U-100, Biobrás) in the evening, at the beginning of the dark cycle, from the 3rd day after STZ injection throughout the experiment. The animals were weighed every 3 days and, when necessary, the insulin dose was adjusted. Control animals (N=7) received a single injection of vehicle (citrate buffer, pH 5.2) into the penile vein 15 days (N=7) before the experiments.

Under pentobarbital anesthesia, the ADNs were isolated and had their spontaneous activity recorded as previously described [12]. The pulsatile arterial pressure was recorded simultaneously with the ADN activity, to ensure that the nerves studied were the ADN. Proximal and distal segments of the left ADN were prepared for light and transmission electron microscopy studies as reported previously [11,13,14]. Morphometry was performed with the aid of the KS 400 software (Kontron 2.0, Eching Bei Muchen, Germany). The investigator was blinded to group identity throughout the morphometric process. Sample morphometry was not used and 100% of the fascicle area was studied.

All nerve samples were processed at once to assure that the alterations observed were not due to artifacts introduced by the histological procedures. The light microscopy study was performed to validate the quality of the histological preparation of the nerves and to perform the light microscopy studies. Only nerves with good histological preservation were used. The fascicle images were collected from semithin transverse sections, stained with 1% toluidine blue, using a digital camera (Axiocam MR5, Carl Zeiss) connected to an IBM PC. With the aid of KS 400 software, the total number of myelinated fibers and the total number of Schwann cells nuclei present in each fascicle was identified by visual inspection and counted. The fascicular area was measured and the myelinated fiber density (fiber/mm²) and the Schwann cell nuclei density (nucleus/mm²) were calculated. Myelinated fiber morphometry was performed as described previously [15,16] and the parameters obtained were axonal area and diameter and total fiber area and diameter. Also, the ratio between the axonal diameter

and total fiber diameter (which indicates the degree of myelination), described as G ratio [17,18], was obtained. Finally, myelin sheath area was calculated for each myelinated fiber measured.

For the ultrastructural studies, thin transverse sections were mounted on Formvar coated 2×1 slot grids, stained with lead citrate and uranyl acetate, and observed with a JEM-1230 transmission electron microscope (JEOL-USA, Inc., Peabody, MA, USA) equipped with a digital camera. Using the image analysis software, the total number of the unmyelinated fibers was counted, and their diameter measured as described [11,19-21]. The density of the unmyelinated fiber was calculated and the ratio between unmyelinated/myelinated fibers was determined. A histogram of the unmyelinated fiber diameter was constructed and separated into class intervals increasing by 0.1 μm. Data are presented as mean ± standard error of mean (SEM).

For the statistical analysis, the Kolmogorov-Smirnov test was applied to verify the normal distribution for weight, biochemical, physiological and morphometric data, using Sigma Stat software, version 3.01 (Jandel Scientific), followed by the Levene test of medians for variance equivalence.

Body weight and blood glucose level data were compared between the 3rd day of injection and the experimental day by the non-parametric test of Wilcoxon for paired samples and among groups by the analysis of variance on Ranks, followed by Tukey's post hoc test, provided that these data did not show normal distribution. The mean arterial pressure (MAP) and heart rate (HR) data between groups were also compared by the analysis of variance on Ranks, followed by Tukey's post hoc test.

Morphometric data that passed the normality and variance equivalence tests were compared by paired Student's t-test (between the proximal and distal segments) and one way ANOVA followed by a Holm-Sidak post hoc test (for segments between groups). Otherwise, proximal and distal segments were compared using the non-parametric test of Wilcoxon for paired samples, while groups were compared by the analysis of variance on ranks, followed by Dunn's post hoc test.

Differences were considered significant when $p < 0.05$.

Results

Biochemical and physiological data

At the beginning of the experiments, there was no difference in body weight between all groups. At the experimental day, all groups showed significant increase in body weight comparing to the beginning of the experiments but STZ animals gained less weight compared to control and compared to insulin treated groups. Blood glucose level was significantly high on both STZ groups (treated and untreated) three days after injection compared to controls. This difference was also observed on the experimental day, but treated animals showed a significant reduction on the blood glucose level compared to the beginning of treatment. Mean arterial pressure was significantly reduced on STZ animals compared to controls and treated animals, with no difference on the heart rate between groups. Numerical data is presented on Table 1.

Morphology

No evident morphological differences were observed between the experimental groups in the light microscopy level, except that the insulin treated nerves seemed to be smaller compared to nerves from the other two experimental groups. The ultrastructural qualitative analysis showed that control nerves present morphological

characteristics similar to the normal ADN described for rats [12]. Nerves from diabetic animals showed some unmyelinated fiber enlargement with signs of swelling and degeneration, but the most striking alteration was observed on the Schwann cells mitochondria, that presented enlargement and clustering formation (Figure 1). For the insulin treated animals, an important thickening of the Schwann cells' basement membrane was present and some myelinated fibers showed thin myelin sheaths (Figure 1). The endoneurial blood vessels ultrastructure was preserved in all nerves from the three experimental groups.

Fascicle morphometry

Table 2 shows the average values for fascicular morphometric parameters of the ADN from control, acute diabetic and treated acute diabetic rats. There were no differences between proximal and distal segments from nerves in the same experimental group. Despite the morphological observation that nerves from treated animals tended to be smaller compared to controls, no differences on the fascicular area were found between groups. Also, there were no differences between groups on the Schwann cells nuclei number and density. Myelinated fiber number was significantly smaller on insulin treated groups, on both segments, compared to controls and to diabetic animals, with no corresponding differences on the myelinated fiber density.

Fiber morphometry

The average area and diameter of the myelinated fibers and respective axons as well as the average myelin sheath area and G ratio for the ADN from the three experimental groups are shown in Table 3. Values from proximal and distal segments are shown. Myelinated axon area and diameter was significantly larger on treated animals, compared to both, controls and acute diabetic groups, on both segments. No other differences were observed between groups for the myelinated fibers morphometric parameters. The ADN average values for unmyelinated fiber number, density, diameter and the unmyelinated/myelinated fiber ratio are shown in Table 4 for proximal and distal segments of nerves from the three experimental groups. No significant differences were found for all parameters between groups. Also, either for myelinated or unmyelinated fibers morphometric parameters, no differences between proximal and distal segments were present in nerves from the same experimental group.

Distribution histograms

Histograms of size distribution of the unmyelinated fibers showed that fibers diameter ranged from 0.1 to 1.2 μm , with a peak at 0.4 μm on proximal segments for the three experimental groups (Figure 2). On the distal segments, fibers also ranged from 0.1 to 1.2 μm but while controls and insulin treated groups showed peaks at 0.4 μm , diabetic animals presented the distribution peak at 0.5 μm with a shift of the distribution to the right.

Discussion

Few literature reports deal with transmission electron microscopy studies of autonomic nerves in diabetes, particularly in early onset of the disease. We investigated the ADN, an important nerve related to cardiovascular reflexes known to be altered in diabetes. Important results from this study include early Schwann cell involvement in diabetes with severe mitochondrial damage. Also, insulin treatment resulted in thickening of the Schwann cells basement membrane.

Alterations on the nerve extracellular matrix in diabetic patients have been investigated and include thickening of the microvasculature

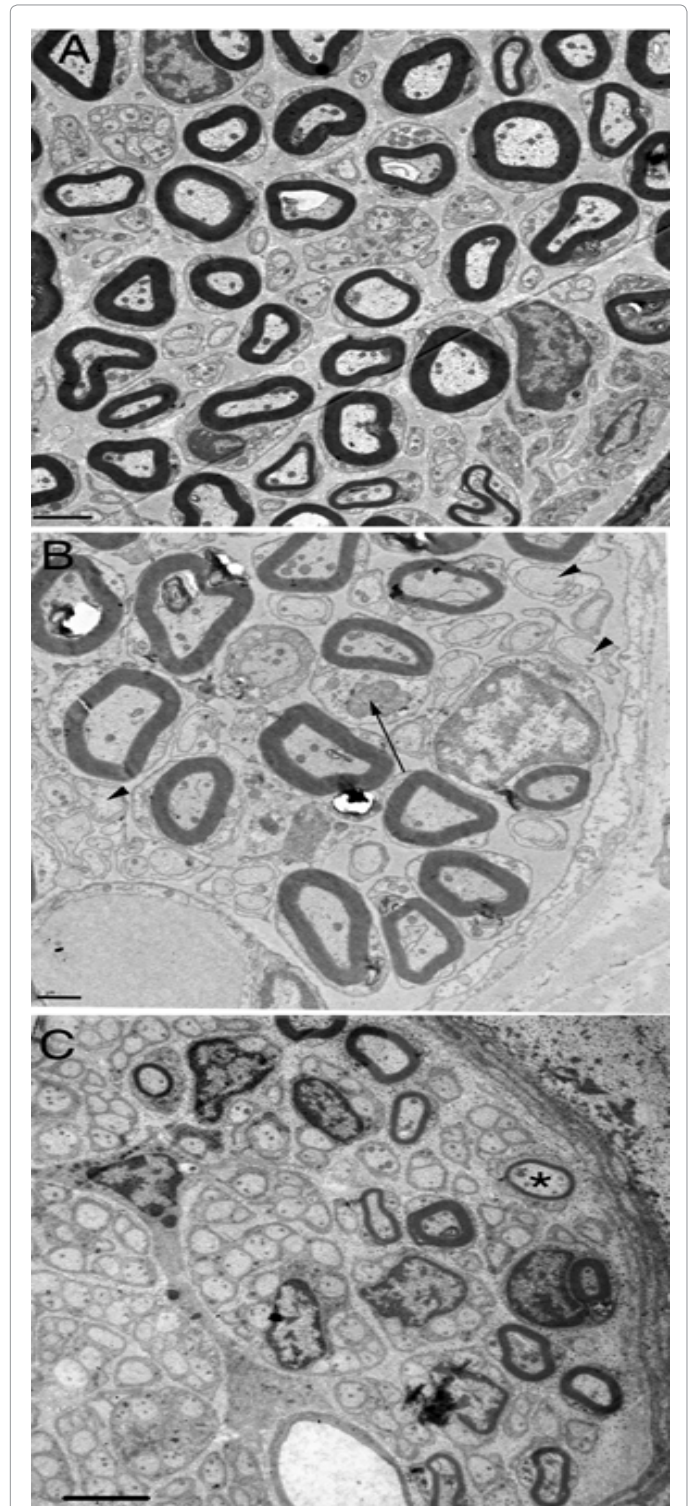


Figure 1: Representative thin cross sections of the aortic depressor nerve (ADN) from control (A), acute diabetic (B) and acute diabetic treated with insulin (C). No morphological ultrastructural alterations were observed in control nerves. Nerves from diabetic animals (B) present enlarged unmyelinated fibers (arrow heads) and enlargement and clustering formation on the Schwann cells mitochondria (arrow). Note that insulin treated animals (C) present an important thickening of the Schwann cells' basement membrane. Some myelinated fibers showed thin myelin sheaths (*). The endoneurial blood vessels ultrastructure was preserved in all nerves from the three experimental groups. Bar = 1 μm .

	Body Weight	Blood Glucose	MAP	HR
Control - 3 days	203 ± 14	85 ± 6 ^{#†}		
STZ - 3 days	201 ± 10	533 ± 27*		
STZ+Ins - 3 days	205 ± 11	538 ± 52*		
Control - 15 days	295 ± 39 ⁺	76 ± 10 [#]	96 ± 8	315 ± 32
STZ - 15 days	232 ± 9 ^{**}	548 ± 61*	69 ± 21*	291 ± 63
STZ+Ins - 15 days	302 ± 20 ^{**}	127 ± 27 ^{**}	87 ± 8	301 ± 15

STZ = diabetic group; STZ+Ins = Diabetic group treated with insulin. * significant difference compared to control group at the same experimental time; # significant difference compared to STZ group at the same experimental time; † significant difference compared to STZ + Ins group at the same experimental time; + significant difference compared to the same group at 3 days.

Table 1: Body weight and blood glucose level on the 3rd day after streptozotocin (STZ) or vehicle injection, and on the experimental day (15 days after injection), together with average mean arterial pressure (MAP) and heart rate (HR) on the experimental day. Data are expressed as mean ± standard error of mean (SEM).

	Control	STZ	STZ+Ins
<i>Proximal Segments</i>			
Fascicular Area (µm ²)	869 ± 93	827 ± 112	721 ± 175
Myelinated Fiber Number	74 ± 8	62 ± 10	32 ± 11 ^{**}
Myelinated Fiber Density (fiber/mm ²)	89790 ± 8763	75462 ± 9057	49558 ± 16999
Schwann Cell Nuclei Number	9 ± 2	9 ± 1	4 ± 1
Schwann Cell Nuclei Density (nucleus/mm ²)	9430 ± 1444	11019 ± 1028	7158 ± 500
<i>Distal Segments</i>			
Fascicular Area (µm ²)	871 ± 59	816 ± 158	868 ± 261
Myelinated Fiber Number	79 ± 8	61 ± 9	32 ± 12 ^{**}
Myelinated Fiber Density (fiber/mm ²)	86473 ± 6897	77819 ± 5787	55277 ± 17835
Schwann Cell Nuclei Number	10 ± 1	9 ± 2	7 ± 1
Schwann Cell Nuclei Density (nucleus/mm ²)	11302 ± 1302	11575 ± 2145	14435 ± 2784

* significant difference compared to control group; # significant difference compared to STZ group.

Table 2: Morphometric parameters of the proximal and distal fascicles of the aortic depressor nerve (ADN) in control, diabetic (STZ) and diabetic treated with insulin (STZ+Ins) groups. Data are expressed as mean ± standard error of mean (SEM).

	Control	STZ	STZ+Ins
<i>Proximal Segments</i>			
Myelinated Fiber Area (µm ²)	4.24 ± 0.32	4.24 ± 0.38	7.00 ± 1.61
Myelinated Fiber Diameter (µm)	1.92 ± 0.09	1.96 ± 0.09	2.26 ± 0.23
Myelinated Axon Area (µm ²)	1.40 ± 0.08	1.34 ± 0.12	2.80 ± 0.52 [#]
Myelinated Axon Diameter (µm)	1.05 ± 0.04	1.05 ± 0.05	1.36 ± 0.09 ^{**}
Myelin Sheath Area (µm ²)	2.83 ± 0.26	2.91 ± 0.33	4.20 ± 1.14
G Ratio	0.55 ± 0.01	0.53 ± 0.02	0.60 ± 0.02
<i>Distal Segments</i>			
Myelinated Fiber Area (µm ²)	4.27 ± 0.20	4.23 ± 0.17	5.92 ± 1.00
Myelinated Fiber Diameter (µm)	1.95 ± 0.06	1.99 ± 0.05	2.17 ± 0.12
Myelinated Axon Area (µm ²)	1.44 ± 0.10	1.29 ± 0.13	2.22 ± 0.17 ^{**}
Myelinated Axon Diameter (µm)	1.08 ± 0.05	1.04 ± 0.13	1.30 ± 0.03 ^{**}
Myelin Sheath Area (µm ²)	2.83 ± 0.13	2.94 ± 0.252	3.71 ± 0.841
G Ratio	0.55 ± 0.01	0.53 ± 0.03	0.60 ± 0.03

* significant difference compared to control group; # significant difference compared to STZ group

Table 3: Morphometric parameters of the proximal and distal segments of the aortic depressor nerve (ADN) myelinated fibers in control, diabetic (STZ) and diabetic treated with insulin (STZ+Ins) groups. Data are expressed as mean ± standard error of mean (SEM).

basement membrane as well as thickening of the perineural cell basement membrane [22-25]. Thickening of the Schwann cells basement membrane was less reported, either in humans [25] or in experimental diabetes [21]. The extracellular matrix in peripheral nerves gives mechanical support to the surrounding cells. It also participates on the regulation mechanisms and interactions mediated by molecules on the surface of the cells [25]. In this way, any structural change on the basement membranes might lead to cellular dysfunction in multiple ways. We are showing that thickening of the Schwann cells basement membrane occurs associated with the onset of insulin treatment. One possible interpretation for this finding is that the animals might have undergone through periods of hypoglycaemia during the treatment. The effects of insulin-induced hypoglycaemia on

peripheral nerves were recently revised [26] and no similar findings to those in our study were described. Thus, it is more likely that the insulin is causing a direct effect on the Schwann cells metabolism and synthesis of surface molecules.

Altered or aberrant mitochondrial morphology have been described in metabolic diseases including diabetes. Mitochondrial phenotype abnormality in sensory neurons, Schwann cells and sympathetic ganglia in diabetes was described [27]. Recently, alterations in axonal mitochondria were also shown in acute experimental diabetes [21]. Hyperglycemia in diabetes triggers nutrient excess in neurons that mediates the phenotype changes in mitochondria [27,28]. We are demonstrating that, at early stages of diabetes, mitochondria from the

	Control	STZ	STZ+Ins
<i>Proximal Segments</i>			
Unmyelinated Fiber Number	269 ± 51	330 ± 97	110 ± 63
Unmyelinated Fiber Density (Fiber/mm ²)	301x10 ³ ± 49x10 ³	389x10 ³ ± 112x10 ³	183x10 ³ ± 88x10 ³
Unmyelinated Fiber Diameter (µm)	0.44 ± 0.04	0.45 ± 0.03	0.43 ± 0.01
Unmyelinated/Myelinated Fiber Ratio	4 ± 1	7 ± 3	7 ± 3
<i>Distal Segments</i>			
Unmyelinated Fiber Number	213 ± 41	261 ± 79	144 ± 65
Unmyelinated Fiber Density (Fiber/mm ²)	227x10 ³ ± 55x10 ³	334x10 ³ ± 86x10 ³	196x10 ³ ± 87x10 ³
Unmyelinated Fiber Diameter (µm)	0.43 ± 0.03	0.50 ± 0.03	0.41 ± 0.04
Unmyelinated/Myelinated Fiber Ratio	3 ± 1	4 ± 1	9 ± 5

* significant difference compared to control group; # significant difference compared to STZ group

Table 4: Morphometric parameters of the proximal and distal segments of the aortic depressor nerve (ADN) unmyelinated fibers in control, diabetic (STZ) and diabetic treated with insulin (STZ+Ins) groups. Data are expressed as mean ± standard error of mean (SEM).

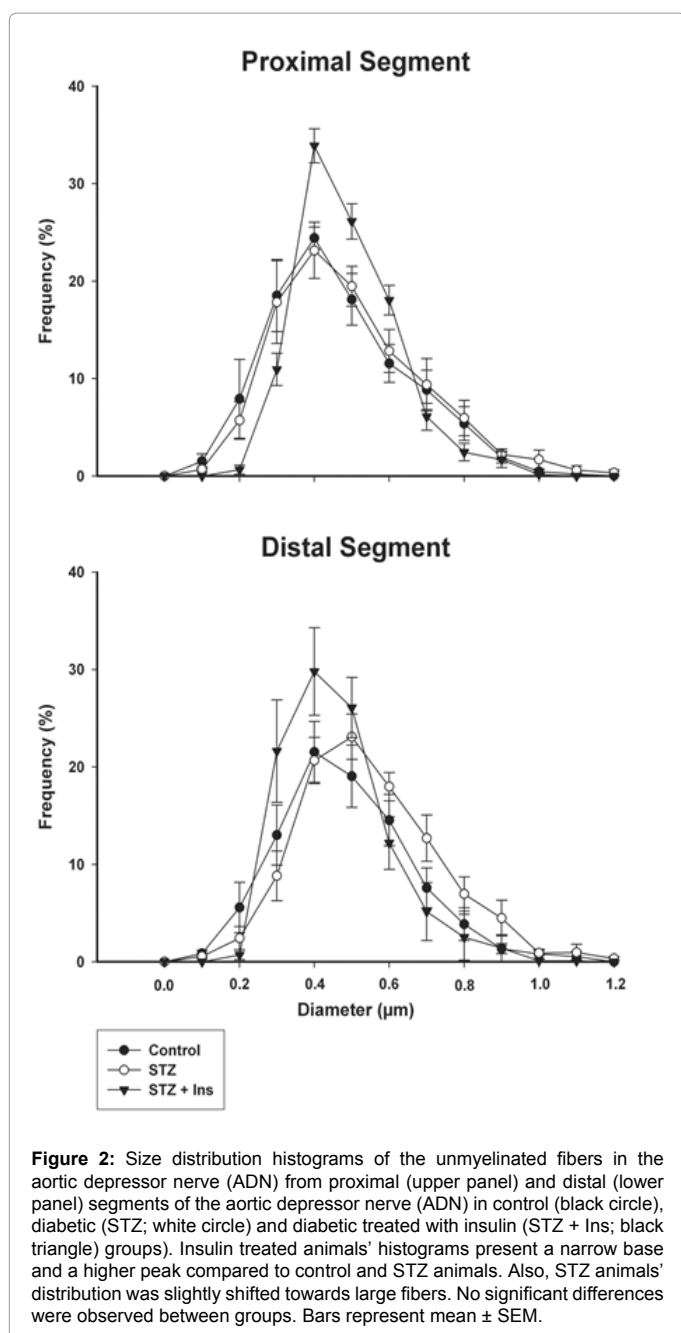


Figure 2: Size distribution histograms of the unmyelinated fibers in the aortic depressor nerve (ADN) from proximal (upper panel) and distal (lower panel) segments of the aortic depressor nerve (ADN) in control (black circle), diabetic (STZ; white circle) and diabetic treated with insulin (STZ + Ins; black triangle) groups. Insulin treated animals' histograms present a narrow base and a higher peak compared to control and STZ animals. Also, STZ animals' distribution was slightly shifted towards large fibers. No significant differences were observed between groups. Bars represent mean ± SEM.

Schwann cells are also affected and this might be related to increased metabolic demand in these cells. Mitochondrial damage may precede axonal degeneration and despite that morphological studies do not provide clear insights into mitochondrial function, it seems reasonable to venture that function will be compromised in mitochondria which are physically different from normal ones [29].

Small fiber neuropathy in diabetic patients is commonly accessed by intraepidermal fiber quantification [30] while transmission electron microscopy studies are rarely performed. In experimental models, a reduction of the myelinated fiber and axon sizes is often described for somatic nerves either by light [31,32] or transmission electron microscopy studies [33]. For the autonomic nerves, small myelinated fibers loss was shown in STZ-model of diabetes [21], suggesting that somatic and autonomic nerves might react in distinct ways to diabetes. We showed that the onset of insulin treatment caused a reduction of the small myelinated fiber number. Since the axon size was significantly larger on insulin treated animals, it is suggestive that the remaining myelinated fibers are the larger ones that shifted the average size to higher values.

The ultrastructure of the phrenic nerve in chronic experimental diabetes [20] showed no differences in number or density of the unmyelinated fibers, similar to our study, despite the important alterations on the endoneurial blood vessels described by those authors. It has been suggested that small fiber alterations could be due to a poor vascularization of the endoneurial space [20,34]. In our study, no morphological alterations were present on the endoneurial blood vessels, pointing to the fact that the small myelinated fiber loss was not related to endoneurial ischemia. Also, it is suggestive that Schwann cells are more sensitive to the insulin treatment and respond readily than the blood vessels cells, in thickening the basement membrane.

Functional alterations of the baroreflex in diabetic rats have been demonstrated and our observation of a decrease in the MAP was also described by others [35-38]. Several hypotheses for this decrease were raised such as reduced cardiac output due to the hypovolemia caused by osmotic diuresis [39], reduced myocardial contractility leading to myocardial dysfunction [40] or the decrease of peripheral resistance [41]. In spite of all morphological alterations in response to insulin treatment, it attenuated the observed reduction in the MAP. This study explored the morphological alterations of the ADN in acute experimental diabetes. One of the limitations of the study is that functional correlates for the morphological findings need further investigation.

Conclusion

Investigation of experimental models of diabetes in early or acute stage of the disease provide relevant information on the physiopathological mechanisms involved in the alterations present in patients with chronic diabetes and its complications. This information may lead to a better understanding of the disease itself and provide background for the development of new approaches to therapeutics. We suggest that insulin treatment alone might have a role on the morphological alterations present in diabetic neuropathy.

Acknowledgments

We thank Mr. Antônio Renato Meirelles e Silva, Experimental Neurology Laboratory and Ms. Maria Tereza P. Magliã, Electron Microscopy Laboratory, School of Medicine of Ribeirão Preto, for excellent technical support. **GRANTS:** Grant sponsor: FAPESP (Fundação de Amparo à Pesquisa do Estado de São Paulo); Grant numbers 2012/00321-0 and 2013/01111-0; Grant sponsor: CNPq (Conselho Nacional de Pesquisa e Tecnologia); Grant number: 300900/2013-9.

References

1. Dyck PJ, Giannini C (1996) Pathologic alterations in the diabetic neuropathies of humans: a review. *J Neuropathol Exp Neurol* 55: 1181-1193.
2. Comi G, Corbo M (1998) Metabolic neuropathies. *Curr Opin Neurol* 11: 523-529.
3. Centers for Disease Control and Prevention. National Diabetes Statistics Report: Estimates of Diabetes and Its Burden in the United States, 2014. Atlanta, GA: U.S. Department of Health and Human Services.
4. Sharma AK, Thomas PK (1999) Animal models: Pathology and Pathophysiology: Diabetic Neuropathy. (2nd edn), WB Saunders Company, Philadelphia.
5. Ewing DJ, Campbell IW, Clarke BF (1980) The natural history of diabetic autonomic neuropathy. *Q J Med* 49: 95-108.
6. Vinik A, Mitchell B (1988) Clinical aspects of diabetic neuropathies. *Diabetes Metab Rev* 4: 223-253.
7. Maeda CY, Fernandes TG, Timm HB, Irigoyen MC (1995) Autonomic dysfunction in short-term experimental diabetes. *Hypertension* 26: 1100-1104.
8. Hicks KK, Seifen E, Stimers JR, Kennedy RH (1998) Effects of streptozotocin-induced diabetes on heart rate, blood pressure and cardiac autonomic nervous control. *J Auton Nerv Syst* 69: 21-30.
9. Carvalho CS, Sato KL, Castania JA, Salgado HC, Nessler RA et al. (2014) Ultrastructural Morphometry of the Aortic Depressor Nerves and Extrinsic Renal Nerves: Similarities and Differences between Mice and Rats. *Anat Physiol* 4:142.
10. Kobayashi M, Cheng ZB, Tanaka K, Nosaka S (1999) Is the aortic depressor nerve involved in arterial chemoreflexes in rats? *J Auton Nerv Syst* 78: 38-48.
11. Oliveira FS, Nessler RA, Castania JA, Salgado HC, Fazan VP (2013) Ultrastructural and morphometric alterations in the aortic depressor nerve of rats due to long term experimental diabetes: effects of insulin treatment. *Brain Res* 1491: 197-203.
12. Fazan VP, Salgado HC, Barreira AA (1997) A descriptive and quantitative light and electron microscopy study of the aortic depressor nerve in normotensive rats. *Hypertension* 30: 693-698.
13. Fazan VP, Júnior RF, Salgado HC, Barreira AA (1999) Morphology of aortic depressor nerve myelinated fibers in normotensive Wistar-Kyoto and spontaneously hypertensive rats. *J Auton Nerv Syst* 77: 133-139.
14. Fazan VP, Salgado HC, Barreira AA (2001) Aortic depressor nerve unmyelinated fibers in spontaneously hypertensive rats. *Am J Physiol Heart Circ Physiol* 280: H1560-1564.
15. Jeronimo A, Jeronimo CA, Rodrigues Filho OA, Sanada LS, Fazan VP (2005) Microscopic anatomy of the sural nerve in the postnatal developing rat: a longitudinal and lateral symmetry study. *J Anat* 206: 93-99.
16. Jeronimo A, Jeronimo CA, Rodrigues Filho OA, Sanada LS, Fazan VP (2008) A morphometric study on the longitudinal and lateral symmetry of the sural nerve in mature and aging female rats. *Brain Res* 1222: 51-60.
17. RUSHTON WA (1951) A theory of the effects of fibre size in medullated nerve. *J Physiol* 115: 101-122.
18. Smith RS, Koles ZJ (1970) Myelinated nerve fibers: computed effect of myelin thickness on conduction velocity. *Am J Physiol* 219: 1256-1258.
19. Sato KL, do Carmo JM, Fazan VP (2006) Ultrastructural anatomy of the renal nerves in rats. *Brain Res* 1119: 94-100.
20. Fazan VP, Rodrigues Filho OA, Jordão CE, Moore KC (2009) Phrenic nerve diabetic neuropathy in rats: unmyelinated fibers morphometry. *J Peripher Nerv Syst* 14: 137-145.
21. Sato KL, Sanada LS, Ferreira Rda S, de Marco MC, Castania JA, et al. (2014) Renal nerve ultrastructural alterations in short term and long term experimental diabetes. *BMC Neurosci* 15: 5.
22. Johnson PC, Brendel K, Meezan E (1981) Human diabetic perineurial cell basement membrane thickening. *Lab Invest* 44: 265-270.
23. Bradley JL, Thomas PK, King RH, Watkins PJ (1994) A comparison of perineurial and vascular basal laminal changes in diabetic neuropathy. *Acta Neuropathol* 88: 426-432.
24. Hill RE, Williams PE (2004) Perineurial cell basement membrane thickening and myelinated nerve fibre loss in diabetic and nondiabetic peripheral nerve. *J Neurol Sci* 217: 157-163.
25. Peltonen JT, Kalliomäki MA, Muona PK (1997) Extracellular matrix of peripheral nerves in diabetes. *J Peripher Nerv Syst* 2: 213-226.
26. Jensen VF, Mølck AM, Bøgh IB, Lykkesfeldt J (2014) Effect of insulin-induced hypoglycaemia on the peripheral nervous system: focus on adaptive mechanisms, pathogenesis and histopathological changes. *J Neuroendocrinol* 26: 482-496.
27. Chowdhury SK, Smith DR, Fernyhough P (2013) The role of aberrant mitochondrial bioenergetics in diabetic neuropathy. *Neurobiol Dis* 51: 56-65.
28. Chowdhury SK, Dobrowsky RT, Fernyhough P (2011) Nutrient excess and altered mitochondrial proteome and function contribute to neurodegeneration in diabetes. *Mitochondrion* 11: 845-854.
29. Sajic M (2014) Mitochondrial dynamics in peripheral neuropathies. *Antioxid Redox Signal* 21: 601-620.
30. Ragé M, Acker NV, Knaapen MWM, Timmers M, Streffer J et al. (2011) Asymptomatic small fiber neuropathy in diabetes mellitus: investigations in intraepidermal nerve fiber density, quantitative sensory testing and laser-evoked potentials. *J Neurol* 258: 1852-1864.
31. Yagihashi S, Kamijo M, Watanabe K (1990) Reduced myelinated fiber size correlates with loss of axonal neurofilaments in peripheral nerve of chronically streptozotocin diabetic rats. *Am J Pathol* 136: 1365-1373.
32. Rodrigues Filho OA, Fazan VP (2006) Streptozotocin induced diabetes as a model of phrenic nerve neuropathy in rats. *J Neurosci Methods* 151: 131-138.
33. Weis J, Dimpfel W, Schröder JM (1995) Nerve conduction changes and fine structural alterations of extra- and intrafusal muscle and nerve fibers in streptozotocin diabetic rats. *Muscle Nerve* 18: 175-184.
34. Parry GJ, Brown MJ (1982) Selective fiber vulnerability in acute ischemic neuropathy. *Ann Neurol* 11: 147-154.
35. do Carmo JM, Huber DA, Castania JA, Fazan VP, Fazan R Jr, et al. (2007) Aortic depressor nerve function examined in diabetic rats by means of two different approaches. *J Neurosci Methods* 161: 17-22.
36. do Carmo JM, Júnior RF, Salgado HC, Fazan VP (2011) Methods for exploring the morpho-functional relations of the aortic depressor nerve in experimental diabetes. *J Neurosci Methods* 195: 30-35.
37. Fazan R Jr, Ballejo G, Salgado MC, Moraes MF, Salgado HC (1997) Heart rate variability and baroreceptor function in chronic diabetic rats. *Hypertension* 30: 632-635.
38. Fazan R Jr, Dias da Silva VJ, Ballejo G, Salgado HC (1999) Power spectra of arterial pressure and heart rate in streptozotocin-induced diabetes in rats. *J Hypertens* 17: 489-495.
39. Kohler L, Boillat N, Lüthi P, Atkinson J, Peters-Haefeli L (1980) Influence of streptozotocin-induced diabetes on blood pressure and on renin formation and release. *Naunyn Schmiedeberg's Arch Pharmacol* 313: 257-261.

40. Hebden RA, Gardiner SM, Bennett T, MacDonald IA (1986) The influence of streptozotocin-induced diabetes mellitus on fluid and electrolyte handling in rats. *Clin Sci (Lond)* 70: 111-117.
41. Low PA, Walsh JC, Huang CY, McLeod JG (1975) The sympathetic nervous system in diabetic neuropathy. A clinical and pathological study. *Brain* 98: 341-356.